IEEE Access
Multidisciplinary | Rapid Review | Open Access Journal

Received May 29, 2020, accepted June 20, 2020, date of publication June 24, 2020, date of current version July 2, 2020.

Digital Object Identifier 10.1109/ACCESS.2020.3004597

A Software-Synchronization Based, Flexible, Low-Cost FMCW Radar

TAO WANG[1], (Senior Member, IEEE), PING LI[1], RUI WANG[1], (Senior Member, IEEE), ZHICHAO SHENG[1], (Member, IEEE), AND LIXUN HUANG[2]

[1]Key Laboratory of Specialty Fiber Optics and Optical Access Networks, Joint International Research Laboratory of Specialty Fiber Optics and Advanced Communication, Shanghai Institute for Advanced Communication and Data Science, Shanghai University, Shanghai 200072, China
[2]School of Computer and Communication Engineering, Zhengzhou University of Light Industry, Zhengzhou 450002, China

Corresponding author: Lixun Huang (shuhlx@163.com)

This work was supported by the Research Grants from the National Natural Science Foundation of China under Grant 61671011 and Grant 61771299.

ABSTRACT With the development of the Internet of Things, FMCW (Frequency Modulated Continuous Wave) radars are widely used in medical treatment, human behavior detection, Internet of Vehicles and UAV (Unmanned Aerial Vehicle) detection. However, the existing systems have some shortcomings, such as high requirements for synchronization signal, lack of flexibility and high design cost. In this paper, to address these problems, a software-synchronization based, flexible, low-cost FMCW radar is proposed. Firstly, the radar uses periodic intermittent slope signal as modulation signal, and analyze echo signal to detect a target with a software synchronization algorithm. Most interestingly, hardware synchronization signal is not needed in the proposed radar as in conventional designs, which greatly facilitate implementation. Secondly, the radar system has a high flexibility due to the use of a software waveform generator and a software data processor. The system is built without expensive integrated chips and equipment, which greatly reduces the design cost. Finally, two groups of experiments under different environments are designed. Through the analysis of the results, it can be seen that the radar system designed in this paper achieves a good accuracy while greatly reduces the design cost and complexity.

INDEX TERMS Frequency modulated continuous wave (FMCW) radars, software synchronization algorithm, flexible, low-cost.

I. INTRODUCTION

A. BACKGROUND

With the rapid development of the Internet of Things, more and more devices based on wireless signals are developed for environmental awareness. Among them are FMCW radars which feature simple structure and wide coverage. Therefore, they have broad application prospects in machine ranging, Internet of Vehicles, human behavior detection and medical treatment [1]–[4]. However, most FMCW radars use continuous ramp signals as modulated signals. Therefore, it is necessary to collect both the beat signal and the synchronous signal at the receiving end, which greatly limits the simplification and low-cost of the equipment.

In this paper, we propose a design of a FMCW radar, which is software synchronization based, flexible and low cost. Firstly, the radar uses periodic intermittent slope signal as modulation signal, and analyze echo signal to detect a target with the software synchronization algorithm. Most interestingly, hardware synchronization signal is not needed in the proposed radar as in conventional designs, which greatly facilitate implementation. Secondly, the radar system uses a software waveform generator and a software data processor to improve the flexibility of the system. The system is built without expensive integrated chips and equipment, which greatly reduces the design cost.

B. RELATED WORK

A survey of the FMCW radars reported recently is listed in Table 1, and we will explain in details their features in the following.

At present, most FMCW radars are designed based on a common hardware signal synchronization mechanism [2]–[10]. Specifically, synchronization signal from

The associate editor coordinating the review of this manuscript and approving it for publication was Muhammad Zakarya.

TABLE 1. Summary of recently reported works for FMCW radars.

Index	Year	Scenario	Signal synchronization mechanism	Equipment	Wave generator software reconfigurable	Signal processing software reconfigurable	Cost
[2]	2019	Detection of human life characteristics	Internal Implementation of Chip	Texas Instrument (TI) mm-wave radar (AWR1443)	No	Yes	Expensive
[3]	2019	Human Continuous Motion Recognition	Hardware Synchronization Signal Required	5.8GHz radar	Unknown	Yes	Medium
[4]	2019	Detection and tracking of pedestrians	Hardware Synchronization Signal Required	Infineon radar chip BGT24MTR12	No	Yes	Low
[5]	2018	Broadband FMCW Radar	Hardware Synchronization Signal Required	Xilinx Virtex VC707	Yes	Yes	Medium
[6]	2018	Detection of Underground Targets	Hardware Synchronization Signal Required	NI-USRP 2932	Yes	Yes	Expensive
[7]	2016	Slow Target Motion Detection	Hardware Synchronization Signal Required	Separate original	No	Yes	Low
[8]	2016	Distance measurement	Hardware Synchronization Signal Required	FPGA	Yes	Yes	Medium
[9]	2014	Indoor positioning and life testing	Hardware Synchronization Signal Required	National Instruments PXIe 1075	Yes	Yes	Expensive
[10]	2019	Vehicle Radar	Software Simulation Implementation	Simulink model	Yes	Yes	None

waveform generator is needed when processing radar echo signal. In [3], [11], this design uses a dual-channel Personal Computer (PC) sound card as the receiving device to acquire the echo signal and synchronization signal of FMCW radar simultaneously. In [2] a mm-wave radar chip (AWR 1443) of Texas Instrument (TI) is used and a 77 GHz FMCW radar is designed based on the chip.

The characteristic of this FMCW radar is that the acquisition of synchronous signal and the analysis of echo signal are completed in the chip. Authors in [6] present a 4.4 GHz FMCW radar design scheme based on a pair of NI-USRP 2932. One of the USRPs acts as a transmitter and the other as a receiver, and the two USRPs synchronize the signals through an external connection.

It is highly desirable to design a FMCW radar with high flexibility. In [5], [8], [12]–[15] FPGA is used as the waveform generator of FMCW radar. The advantage of this scheme is that it can generate arbitrary modulation waveform simply and conveniently by programming. Authors in [4], [7] use discrete originals to build waveform generator.

This design scheme is relatively simple, but loses the possibility of software reconfiguration. If different modulation waveforms are to be produced, we need to replace the original parts with different parameters, which greatly reduces the flexibility of radar system. In [2]–[18], software estimations are used in the analysis of radar echo signals. In [2], [3], [6] PC is used for software estimation, while in [4], [16] MCU is used for the software estimation.

It is also highly attractive to design a FMCW radar with low cost. USRPs from National Instruments Corporation (NI) are used in [6], [19], [20]. With LabVIEW [21], a radio system for detecting underground targets has been successfully built. However, such a FMCW radar system is expensive. Authors in [9] implement a FMCW radar system for indoor positioning and life perception by using National Instruments PXIe 1075 combined with radio frequency module. The design cost is quite high. Furthermore, authors in [5], [8], [11] present the use of FPGA as the signal generation module. This scheme improves the flexibility and reduces the design cost of the system to a certain extent.

C. OUR CONTRIBUTIONS

From the above analysis of related works, it can be seen that a highly flexible and low-cost FMCW radar is highly desirable. Motivated by this consideration, a FMCW radar system is proposed in this paper. In short, the system features the following characteristics:

1) The FMCW radar does not need hardware synchronization signal by designing a special modulation waveform and a software-based synchronization algorithm. Compared

with the previous work to use a dual-channel PC sound card, the radar system designed in this paper only needs to use a single-channel PC sound card to meet the design requirements. It reduces the synchronization requirement of receiving equipment and further reduces the cost and complexity of system design.

2) Furthermore, this paper uses a popular Arduino microprocessor as the software programmable waveform generator, which improves flexibility and reduces cost. One of the advantages of software programmable waveform generator is that it can design modulation signals with different parameters according to actual needs, so as to facilitate comparative experiments of different modulation waveforms.

3) Moreover, the radar system in this paper uses a single-channel PC sound card for data acquisition. The specific parameters such as sampling rate and sampling time of sound card can be set conveniently by using MATLAB directly. The beat signal collected by PC sound card can be used to analyze and calculate the distance and speed information of the current target directly in MATLAB, and can also be stored for later analysis.

Compared with previous works, the proposed radar has low implementation cost since it does not need expensive integrated chips and equipment as in conventional designs.

The rest of this paper is structured as follows. In the next section, the hardware design of the FMCW radar system is introduced. In Section III, the modulation waveform and signal processing algorithm adopted in this paper is introduced in detail. In Section IV, two groups of experiments and results analysis are given. Finally, conclusions are given.

II. HARDWARE DESIGN OF THE RADAR SYSTEM

The hardware design of the proposed FMCW radars mainly includes two parts: a signal generation and transmission part and a signal reception and processing part, as described in Figure. 1.

A. HARDWARE DESIGN OF SIGNAL GENERATION AND TRANSMITTING PART

The signal generation and transmission part is mainly composed of an Arduino nano, a DA (digital to analog) module, a VCO (Voltage Controlled Oscillator) module, a power amplifier module, a power distribution module and a transmitting antenna. In order to realize the programmability of the transmitting signal, Arduino nano is selected as the signal generator in this paper, which improves the flexibility of the radar system. Digital slope signals (such as sawtooth wave, triangular wave, etc.) are generated by using Arduino nano. The digital signals are converted into analog signals through our self-designed DA module, and the VCO is controlled to generate FMCW signal needed by the radar system. The FMCW signal produced by the VCO is divided into two equal-power signals by the power divider, one is sent to the transmitting antenna to radiate outward, the other is sent to the frequency mixer of receiving and processing part as local oscillator signal.

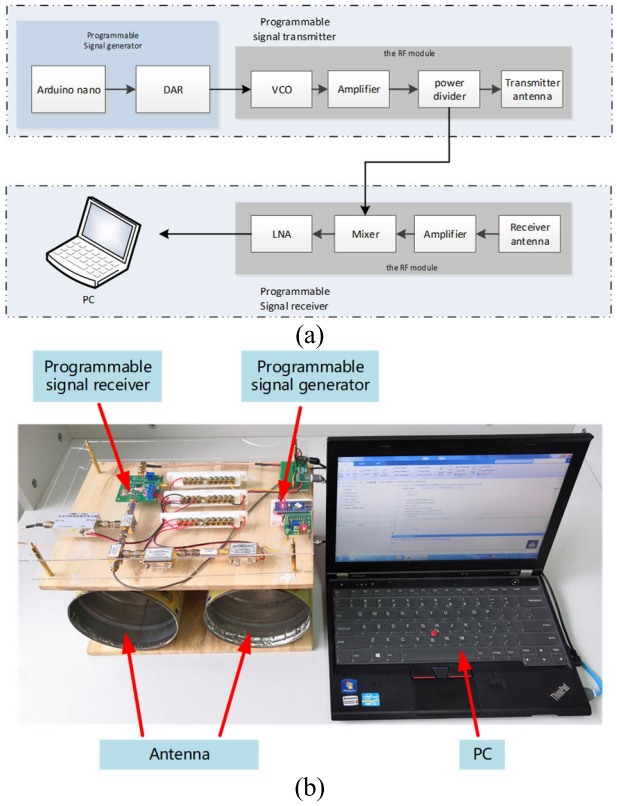

FIGURE 1. Hardware design of FMCW radar. (a) System block diagram. (b) Radar prototype.

B. HARDWARE DESIGN OF SIGNAL RECEIVING AND PROCESSING

The signal receiving and processing part is mainly composed of a receiving antenna, a low noise power amplifier module, a frequency mixer module, a LNA (Low Noise Amplifier) module and a PC. The echo signal received by the radar receiving antenna is amplified and mixed with the local oscillator signal in the frequency mixer module to get the desired beat signal.

Because the beat signal output by direct mixing contains a lot of high frequency interference, it needs to be filtered. In this paper, a self-designed LNA module is adopted. The LNA module is mainly composed of a fourth-order Butterworth low-pass filter and an amplifier, which can filter out the high-frequency interference in the beat signal very well.

The beat signal processed by the LNA module is collected by the PC sound card. Previous radar system designs need to use a dual-channel PC sound card to collect a beat signal and a synchronization signal at the same time, as in [11]. The dual-channel sound card is rarely used in recent PCs, which directly leads to the lack of universal applicability of this radar system. This paper uses a unique design scheme to solve this problem, and realizes the radar system design based on a single channel PC sound card acquisition, which will be introduced in the next chapter. Most interestingly, the sampling time and sampling rate of the PC sound card are flexible and programmable. The data collected by the PC

sound card can be processed in real time in PC and stored for later analysis.

III. DSP DESIGN OF THE RADAR SYSTEM

The software design also includes two parts: the programmable signal generation part and the programmable signal processing part. Software programmability is a major feature of the radar system designed in this paper, which has a high degree of flexibility and reconfigurability. In the past design of FMCW radar system, the beat signal and the synchronization signal need to be collected at the same time, which requires high cost of hardware. To solve this problem, this paper proposes a method of combining the periodic intermittent slope signal with the software synchronization algorithm to design a FMCW radar system without hardware synchronous signal.

A. SOFTWARE PROGRAMMABLE SIGNAL GENERATION PART

The main function of the software programmable signal generation part is to generate the slope signal needed by the FMCW radar system. In this paper, the popular Arduino nano is chosen as the output signal controller, and different modulation waveforms can be flexibly selected as the control signal of the VCO module according to the needs of the actual test environment.

In this paper, a special modulation waveform is designed, which is composed of two parts: a periodic sawtooth wave and a periodic direct current (DC) part. In this paper, it is called periodic intermittent sawtooth wave signal, as shown in Fig. 2-(a). The specific mathematical expressions are as follows:

$$s(t) = \begin{cases} -\dfrac{s_{max}}{t_2} * (t - nT - t_1) + s_{max} \\ nT + t_1 \le t \le (n+1)T, \qquad n = 0, 1, 2, \ldots \\ 0, \qquad\qquad\qquad\qquad other \end{cases} \tag{1}$$

Respectively, s_{max} represents the maximum output amplitude of the signal generator, t_1 represents the duration of direct current signal, t_2 represents the duration of sawtooth signal, $T = t_1 + t_2$ is the period of the modulated signal, and n and k are integers. Correspondingly, the sawtooth wave signal can also be replaced by a triangular wave signal, which is called periodic intermittent triangular wave signal, as shown in Figure. 2-(b). The specific mathematical expressions are as follows:

$$s(t) = \begin{cases} \dfrac{s_{max}}{t_2/2} * (t - nT - t_1), \\ nT + t_1 \le t < (n+1)T - \dfrac{t_2}{2}, \quad n = 0, 1, 2, \ldots \\ -\dfrac{s_{max}}{t_2/2} * (t - nT - t_1) + 2 * s_{max}, \\ nT + t_1 + \dfrac{t_2}{2} \le t \le (n+1)T, \quad n = 0, 1, 2, \ldots \\ 0, \quad other \end{cases} \tag{2}$$

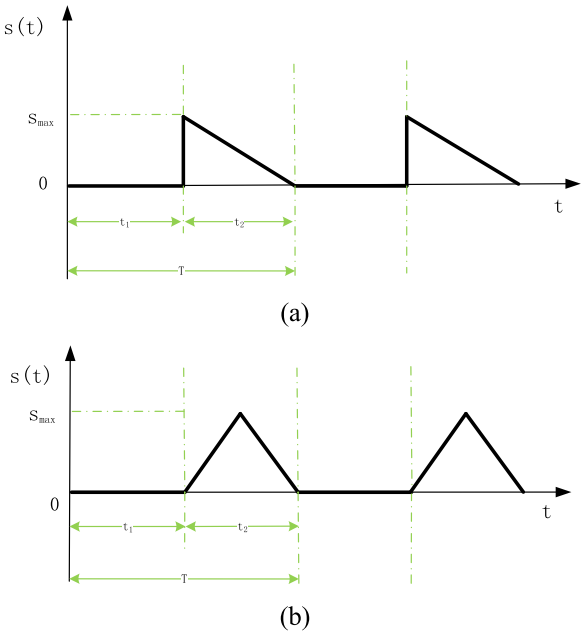

FIGURE 2. The Ramp signal for FMCW radar. (a) Periodic intermittent sawtooth wave signal. (b) Periodic intermittent triangular wave signal.

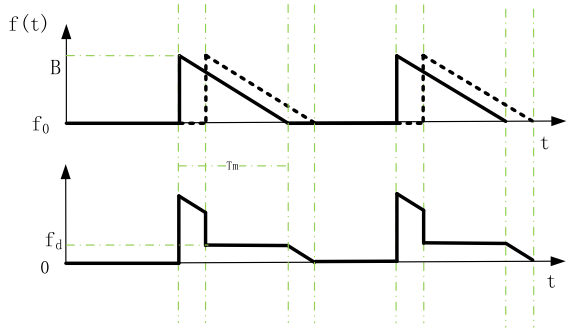

FIGURE 3. The periodic intermittent sawtooth signal and the beat signal.

The reason for choosing this kind of signal as the modulation signal is to facilitate the software synchronization algorithm at the signal processing part.

FMCW radar calculates the frequency difference between the transmitting signal and the echo signal to obtain the distance from the radar to the target. In this paper, a periodic intermittent sawtooth signal is used as the transmitting signal, and the operation principle and process are shown in Fig. 3.

As shown in Fig. 3, the instantaneous frequency of the reflected signal (solid line) of FMCW radar can be expressed as:

$$f_t = f_0 + \frac{B}{T_m} t \tag{3}$$

Respectively, B represents the bandwidth of the radar, f_0 represents the basic frequency of transmitting signal, $T_m = t_2$ represents the duration of sawtooth signal and t is the time. The echo signal (dotted line) is similar to the transmitting signal with an additional delay and the frequency of the echo

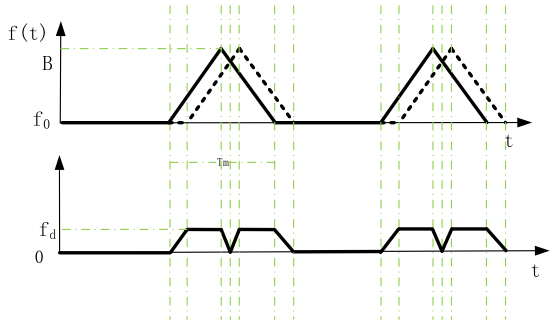

FIGURE 4. The periodic intermittent triangular signal and the beat signal.

signal is:

$$f_r = f_0 + \frac{B}{T_m}\left(t - \frac{2R}{C}\right) \tag{4}$$

where, R represents the distance between the target and the radar and C represents the speed of electromagnetic wave in air. The frequency difference between the transmitted signal and the echo signal is as follows:

$$f_d = f_t - f_r = \frac{2BR}{T_m C} \tag{5}$$

where, f_d represents the beat signal, the target range formula of FMCW radar based on intermittent sawtooth wave is as follows:

$$R = \frac{T_m C f_d}{2B} \tag{6}$$

Correspondingly, when using periodic intermittent triangular wave signal as modulation waveforms, the operation principle and process are shown in Fig. 4, and the formula is as follows:

$$R = \frac{T_m C f_d}{4B} \tag{7}$$

B. SOFTWARE PROGRAMMABLE SIGNAL PROCESSING PART

The main function of the software programmable signal processing part is to collect and analyze the beat signal output by the mixer, and extract the target distance or speed information from it. The specific signal processing process is described as Fig. 5. Unlike the previous design in [11], the radar system designed in this paper does not need to collect synchronous signals, but only collects beat signal. The common PC sound card is used in the acquisition equipment. The sampling rate and sampling time of the sound card can be programmed according to the specific application scenario.

Because the radar system designed in this paper has no hardware synchronization signal, the processing method to capture beat signal is also different from previous works. The first step is to detect the start-point of the signal so as to extract the useful echo signal. In order to achieve better results in signal start-point detection, this paper designs a software synchronization algorithm. Next, the process of signal start-point detection will be introduced in detail.

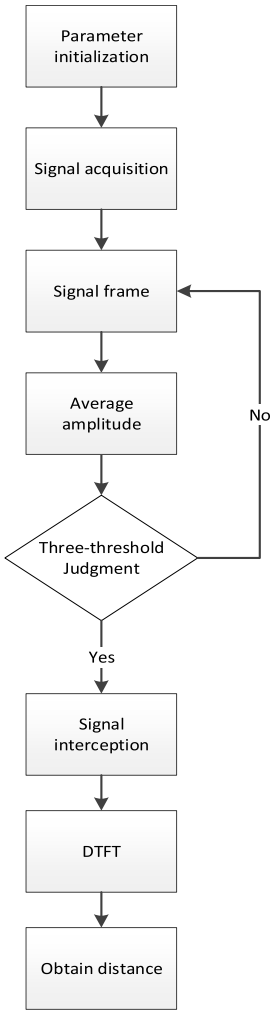

FIGURE 5. The program process of the receiver.

The proposed three-threshold synchronization algorithm is a heuristic algorithm based on signal amplitude characteristics. The input signal of the algorithm is a continuous signal of $2T$ duration collected by sound card. Assuming the sampling rate is R, the number of discrete sampling points corresponding to this signal is $N = 2RT$, which are expressed as $\{r(1), r(2), \ldots, r(N)\}$.

Since the starting time of the acquisition signal is random when the sound card is called, the waveform of $\{r(1), r(2), \ldots, r(N)\}$ may be similar to that of Case (a) or Case (b) as shown in Fig. 6. In any case, the sampled signal contains two parts: the low-amplitude part, which is due to the DC part of the modulation signal, the high-amplitude part, which is due to the slope part of the modulation signal. In Case (a), the sampled signal starts from the low-amplitude part, while in Case (b), the sampled signal starts from the high-amplitude part.

The goal of the synchronization algorithm is to extract a complete useful signal from the sampled signal and provide it to the subsequent parameter estimation algorithm. In Case

(a), the algorithm extracts high-amplitude part signal sampling from start-point 2. In Case (b), the algorithm extracts high-amplitude part signal sampling from start-point 1.

In order to achieve the above objectives, the algorithm adopts an iterative detection method based on three thresholds. In the k-th iteration, it detects whether time k is the starting point of the desired signal. Specifically, a frame signal $\{r(k), r(k+1), \ldots, r(k+L-1)\}$ with length L starting from time k is extracted, and then their average amplitudes are calculated:

$$\overline{a}(k) = \frac{1}{L} \sum_{n=k}^{k+L-1} |r_k(n)| \tag{8}$$

Then, update the statistics in turn: $c1$, $c2$, $c3$. Their roles and renewal methods are as follows:

(1) The function of $c1$ is to record the cumulative number of times that the average amplitude of the signal frame is less than H from the first iteration up to now. The update method of $c1$ is as follows:

$$c1 = \begin{cases} c1+1, & \overline{a}(k) < H \\ 0, & \{c3 > h3\} \, or \, \{c1 > h1 \, and \, c2 > h2\} \\ c1, & other \end{cases} \tag{9}$$

(2) The function of $c2$ is to record the cumulative number of times that the average amplitude of signal frame is higher than that of H from $c1 > h1$ up to now. The update method of $c2$ is as follows:

$$c2 = \begin{cases} c2+1, & \overline{a}(k) > H \, and \, c1 > h1 \\ 0, & c1 > h1 \, and \, c2 > h2 \\ c2, & other \end{cases} \tag{10}$$

(3) The function of $c3$ is to record the cumulative number of times that the average amplitude of signal frame is higher than that of H from the beginning of $c1 < h1$ up to now. The update method of $c3$ is as follows:

$$c3 = \begin{cases} c3+1, & \overline{a}(k) > H \, and \, c1 < h1 \\ 0, & \{c3 > h3\} \, or \, \{c1 > h1 \, and \, c2 > h2\} \\ c3, & other \end{cases} \tag{11}$$

The function of threshold H is to distinguish whether the current frame belongs to a high-amplitude part or a low-amplitude part, and its value is determined by the average amplitude difference between the two parts. The function of threshold $h1$ is to determine whether the low-amplitude part of the signal is detected successfully until the current frame, if $c1 > h1$ indicates success. Its value is determined by the length $n1$ of the low-amplitude part. The function of threshold $h2$ is to determine whether the high-amplitude part of the signal is detected successfully until the current frame, if $c2 > h2$ indicates success. Its value is determined by the length $n2$ of the high-amplitude part. The function of threshold $h3$ is to judge whether the current frame is an abnormal frame

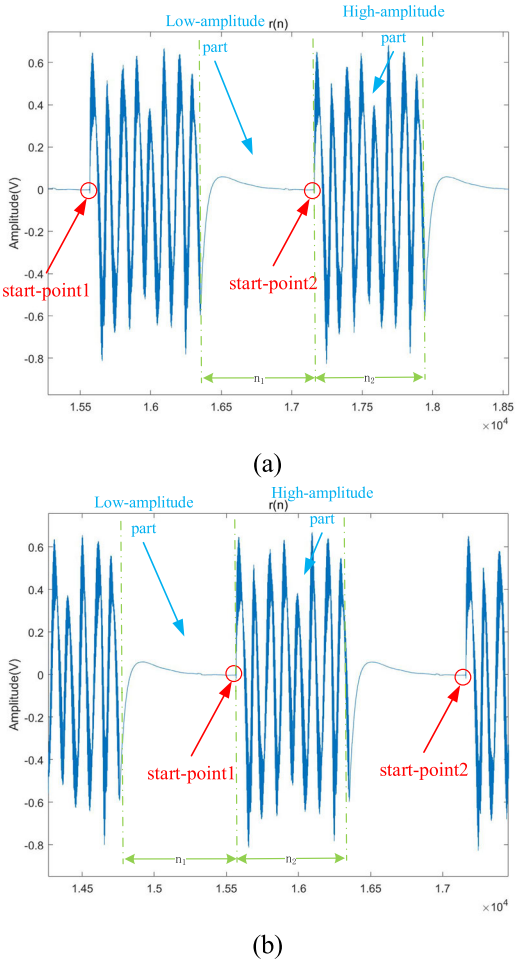

FIGURE 6. Signal diagrams collected by sound card. (a) The signal starts at the low amplitude part. (b) The signal starts at the high amplitude part.

(abnormal frame means that when the oscillation frequency of high-amplitude part decreases, the frame near the zero-crossing point shows the characteristics of low-amplitude part, that is, the average amplitude is lower than threshold H), if $c3 > h3$ means that the current frame is an abnormal frame. Its value is determined by the characteristics of signal noise. The presence of abnormal frames can lead to erroneous detection results, as shown in Fig. 7-(b), where p points to a point in the high-amplitude part.

Finally, the three-threshold synchronization algorithm is used to determine whether k is a start-point. Specifically, if the following formula is satisfied:

$$p = \begin{cases} k, & c1 > h1 \, and \, c2 > h2 \\ 0, & other \end{cases} \tag{12}$$

Then determine that k is the start-point and end the iteration. As Fig. 7- (a) shows, p points to the signal endpoint. Otherwise, the $k+1$ iteration is continued.

In order to understand the proposed three-threshold synchronization algorithm, the pseudo-code of the algorithm is given below, which is summarized as in Table 2.

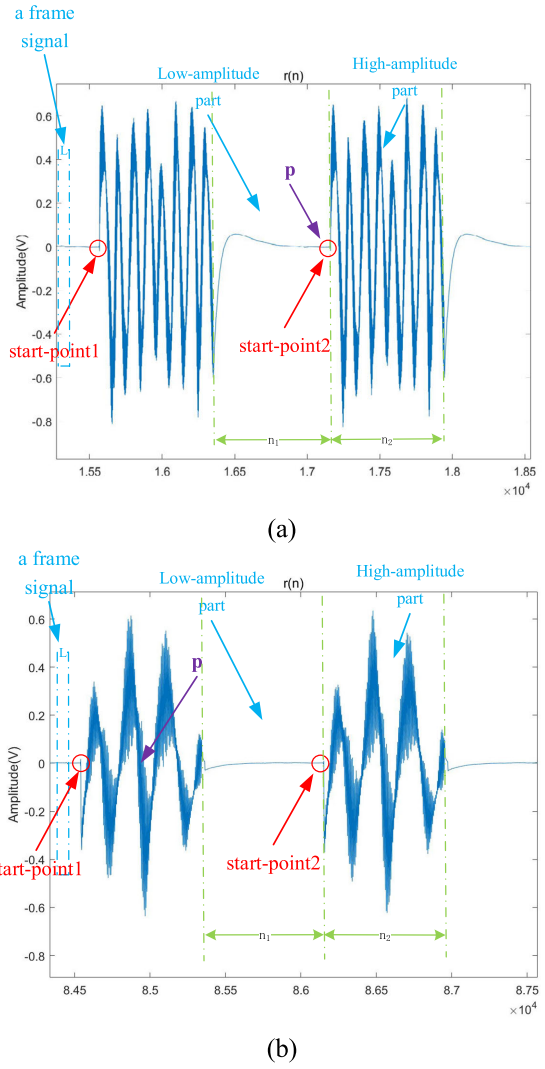

FIGURE 7. Scenario of start-point detection of beat signal. (a) Correctly detection. (b) Error detection.

In order to verify the performance of the three-threshold synchronization algorithm proposed in this paper, we compare it with the variance based synchronization algorithm. In addition, we consider the robustness of algorithms under different SNR conditions. The experimental results are shown in Fig. 8.

From Fig. 8, we found that both algorithms have poor performance and their accuracy is around 5%, when SNR is less than −5dB. When SNR is between −5dB and 0dB, the performance of the algorithm improves significantly, reaching about 80%. After SNR exceeds 20dB, the accuracy rate remains very close to 100%. The performance of the variance based synchronization algorithm is better than that of the proposed algorithm when SNR is greater than 10dB and less than 20dB. However, when SNR is less than 10dB, the performance of this algorithm is not as good as the algorithm proposed in this paper. In addition, we also analyzed the time complexity of two algorithms. The experimental results are shown in Fig. 9.

TABLE 2. Three threshold synchronization algorithm.

Algorithm 1 Three Threshold Synchronization Algorithms
Input: Signal samples $r(1)$, $r(2)$, ..., $r(N)$ captured by the sound card
Output: Signal start-point index p
/*Parameter initialization*/;
$c1 = 0$, $c2 = 0$, $c3 = 0$;
Initialize $h1$, $h2$,$h3$ and H according to training in advance;
for $(k = 1; k \leqslant N - L, k{+}{+})$ **do**
  Construct the k-th signal frame $r(k), r(k-1), ..., r(k-L+1)$;
  Compute $\bar{a}$(k) as the average amplitude of the k-th signal frame;
  if $\bar{a}$(k) $<H$ **then**
    $c1 = c1 + 1$;
  end if
  if $\bar{a}$(k)$>H$ **then**
    if $c1 > h1$ **then**
      $c2 = c2 + 1$;
    end if
    if $c1 < h1$ **then**
      $c3 = c3 + 1$;
    end if
  end if
  if $c3 > h3$ **then**
    $c1 = 0, c3 = 0$;
  end if
  if $c2 > h2$ and $c1 > h1$ **then**
    $p = k$, Break;
  end if
end for
Output p as the start point of the oscillation part of the signal;

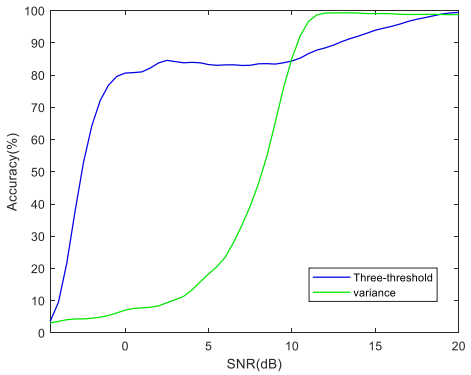

FIGURE 8. Performance comparison of two synchronization algorithms under different SNRs.

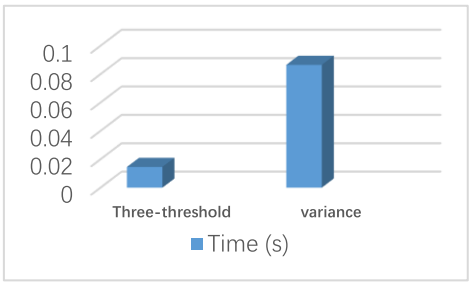

FIGURE 9. Comparison of time complexity of two synchronization algorithms.

As shown in the Fig. 9, we found that the synchronization algorithm proposed in this paper has lower time complexity. In conclusion, the heuristic synchronization algorithm proposed in this paper can better solve the interception of useful echo signal.

After the software synchronization algorithm processing, we intercept a period of signal starting from the detected start-point, which is the desired beat signal. There are many ways to extract target distance information from the beat signal, such as FFT, DTFT etc. Considering the actual situation, the

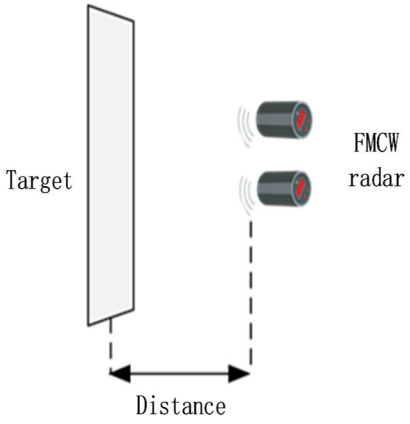

(a)

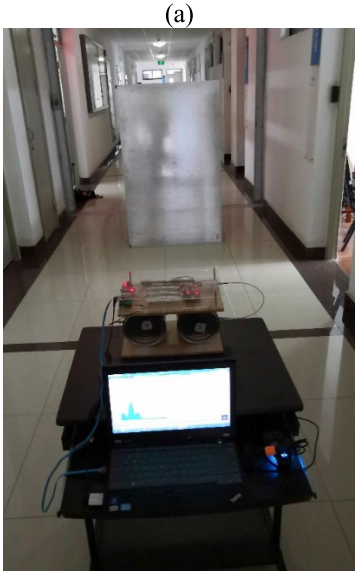

(b)

FIGURE 10. Scene of the distance measurement experiment. (a) Illustration of the experiment. (b) Set up of the experiment.

beat signal period of the FMCW radar system designed in this paper is in the scale of milliseconds. If FFT is used to process data in measuring range, there will be a very serious fence effect, which directly leads to reduction of ranging accuracy. Therefore, this paper chooses DTFT for subsequent processing to improve the measurement accuracy of radar. The mathematical expression of DTFT is as follows [11]:

$$X(e^{j\omega}) = \sum_{n=-\infty}^{\infty} x\,(n) * e^{-j\omega n} \tag{13}$$

After DTFT processing, the frequency domain diagram of the beat signal can be obtained. The frequency corresponding to the maximum peak value is the target beat frequency. Finally, the target distance can be calculated by the distance formula.

IV. EXPERIMENTS AND PERFORMANCE RESULTS

In order to verify the feasibility of FMCW radar system in this paper, two groups of experiments under different

TABLE 3. Experiments using related parameter tables.

Parameter	Value	
	Sawtooth wave	Triangular wave
Amplitude (V)	0-2.35	0-2.49
Period (ms)	80	100
Bandwidth (MHz)	103.87	110.06
Sampling rate of sound card	16000	
Electromagnetic wave velocity (m/s)	3*10^8	

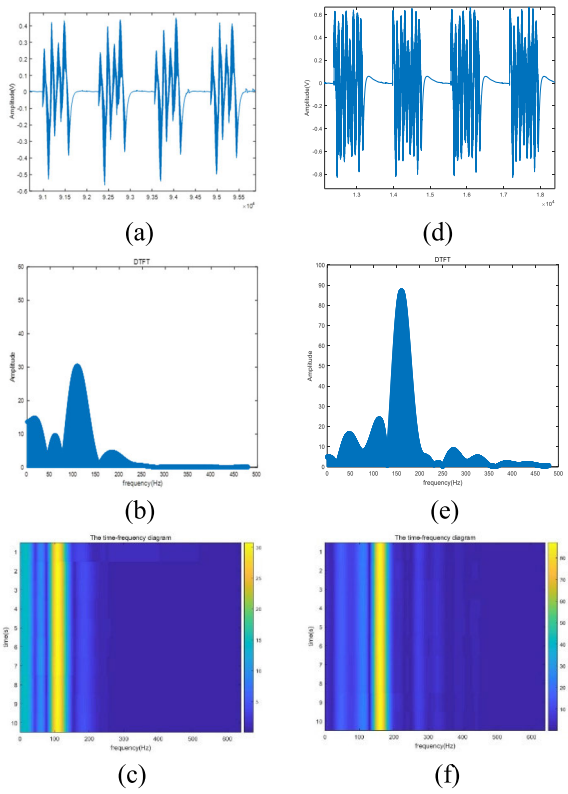

FIGURE 11. The result of laboratory experiment. (a) The beat signal of 3m distance by sawtooth wave. (b) The spectrum magnitude of 3m distance by sawtooth wave. (c)The time-frequent diagram of 3m distance by sawtooth wave. (d) The beat signal of 2.5m distance by triangle wave. (e) The spectrum magnitude of 2.5m distance by triangle wave. (f)The time-frequent diagram of 2.5m distance by triangle wave.

environments are designed: 1) Indoor corridor environment; 2) Outdoor parking environment.

A. INDOOR CORRIDOR ENVIRONMENT

The test environment of FMCW radar is in corridor environment. The test scenario of the corridor is shown in Fig. 10. The target of this test is a 1 × 1.5m metal plate. During the test, the metal plate is moved from near to far, and the distance is measured by the FMCW radar and the data is recorded. The parameters selected for this test are shown in Table 3.

By using the following formula (6) and (7), the required distance information can be calculated from the beat signal.

The signal waveform received by FMCW radar is recorded in the experiment as shown in Fig. 11. Fig. 11(a) shows the real-time beat signal returned by the FMCW radar when

FIGURE 12. Outdoor experimental scene.

TABLE 4. Summary of laboratory corridor test results.

Distance (m)	Modulating waveform	Theoretical beat frequency (Hz)	Actual beat frequency (Hz)	Measuring distance (m)	Error
1.75	Triangular	48.47	50.69	1.83	4.5%
	Sawtooth	60.59	57.56	1.66	5.1%
2.5	Triangular	69.25	70.63	2.55	2%
	Sawtooth	86.56	87.86	2.54	1.6%
3	Triangular	83.09	85.03	3.07	2.3%
	Sawtooth	103.87	100.75	2.91	3%
4.5	Triangular	124.64	117.44	4.24	5.8%
	Sawtooth	155.81	153.73	4.44	1.3%
5	Triangular	138.49	130.73	4.72	5.6%
	Sawtooth	173.12	167.23	4.83	3.4%

measuring static targets 3 m away using periodic intermittent sawtooth waves as modulation waveforms. By analyzing the time-domain waveform of the beat signal, it can be concluded that the signal has obvious periodicity, which is determined by the modulation waveform. The periodic intermittent sawtooth wave signal used in this paper includes the DC part and the sawtooth wave part, which correspond to the steady state part and the oscillation part of beat signal respectively.

In order to extract desired distance information from beat signal, DTFT transform is needed to convert beat signal from time domain to frequency domain, as shown in Fig. 11-(b). From the figure, we can see that there are several peaks in the frequency domain of beat signal. We only need to get the maximum amplitude signal. The frequency value corresponding to the maximum amplitude is the required beat signal value. Other peak signals may be caused by FMCW radar spectrum leakage and other reflections.

In order to illustrate the result clearly, this paper draws the corresponding time-frequency chart in Fig. 11-(c). In addition, the y-axis, x-axis, color represent frequency, time, and amplitude of DTFT. The Fig. 11-(d, e, f) are the time domain diagrams, frequency domain diagrams and time-frequency diagrams of beat signal when FMCW radar uses periodic intermittent triangular waves as modulation waveforms to measure 2.5m far-static targets.

In indoor corridor environment, five groups of test experiments with different distances were designed. The target

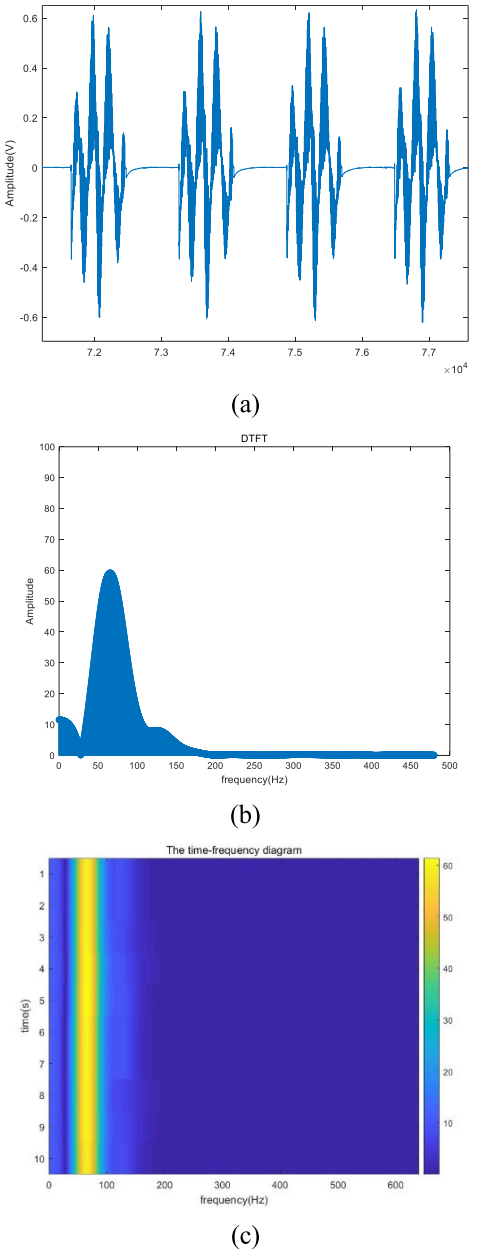

FIGURE 13. The result of laboratory experiment. (a) The beat signal of 2m distance by sawtooth wave. (b) The spectrum magnitude of 2m distance by sawtooth wave. (c)The time-frequent diagram of 2m distance by sawtooth wave.

distances were 1.75m, 2.5m, 3m, 4.5m and 5m, respectively. The periodic intermittent sawtooth wave and the periodic intermittent triangular wave are used as modulation waveforms for each group of experiments at different distances. There are 10 groups of experiments. The test results of FMCW radar at different distances are shown in Table 4.

B. OUTDOOR PARKING ENVIRONMENT

The test environment of FMCW radar is chosen in the an outdoor parking lot. FMCW is often used as vehicle-borne radar to measure the distance between vehicles. For the convenience of experiment, the parking lot is chosen as the

TABLE 5. Summary of outdoor parking test results.

Distance (m)	Modulating waveform	Theoretical beat frequency (Hz)	Actual beat frequency (Hz)	Measuring distance (m)	Error
1	Sawtooth	34.62	34.28	0.99	1%
2	Sawtooth	69.25	72.02	2.08	4%
2.5	Sawtooth	86.56	87.59	2.53	1.2%
3	Sawtooth	103.87	102.86	2.97	1%
4	Sawtooth	138.49	142.31	4.11	2.75%

experimental environment. The specific experimental scenario is shown in Fig. 12. The experimental parameters are in agreement with those of the above experiments.

The signal waveform received by FMCW radar is recorded in the experiment as shown in Fig. 13. In the outdoor parking environment, this paper designs five groups of test experiments with different distances. The target distances are 1m, 2m, 2.5m, 3M and 4m, respectively. Using periodic intermittent sawtooth wave as modulation waveform, five groups of test experiments were carried out. The test results of FMCW radar at different distances are shown in Table 4.

From the experimental results of two groups, the single-channel signal acquisition FMCW radar designed in this paper has a high ranging accuracy. Even if there is no synchronous signal, the experimental results have comparable accuracy as in the literature [11], which shows that it can achieve high accuracy while reducing the complexity of the equipment. Of course, the advantage of software programmable FMCW radar is that users can design specific modulation signal to receive and process algorithm according to the realistic test requirements.

V. CONCLUSIONS

This paper presents a FMCW radar system with software synchronization, high flexibility and low cost. More importantly, this radar is free from the shackles of hardware synchronization signal by means of intermittent ramp signal and synchronization algorithm. Firstly, the radar system uses the periodic intermittent slope signal as a modulation signal, and achieves the data processing method with the software synchronization algorithm. Hardware synchronous signal is not needed for the proposed radar. Then, the radar system uses a programmable signal generator and a software data processor to improve the flexibility of the system. Moreover, the system is built without expensive integrated chips and equipment, which greatly reduces the design cost. Finally, two groups of experiments under different environments are designed. Through the analysis of the results, it can be seen that the radar system designed in this paper attains a good accuracy while greatly reduces the design cost and complexity. Simplified hardware circuit design and flexible software algorithm design guarantees the FMCW radar can meet the needs of various applications.

In future research, we will continue to optimize the existing FMCW radar design scheme for further simplification, and consider to build an integrated ranging and communication system.

REFERENCES

[1] S. Scherr, R. Afroz, S. Ayhan, S. Thomas, T. Jaeschke, M. Pauli, N. Pohl, and T. Zwick, "Target evaluation for high accuracy 80 GHz FMCW radar distance measurements," in *Proc. IEEE Top. Conf. Wireless Sensors Sensor Netw. (WiSNet)*, Jan. 2017, pp. 11–14.

[2] M. Alizadeh, G. Shaker, J. C. M. D. Almeida, P. P. Morita, and S. Safavi-Naeini, "Remote monitoring of human vital signs using mm-wave FMCW radar," *IEEE Access*, vol. 7, pp. 54958–54968, 2019.

[3] C. Ding, H. Hong, Y. Zou, H. Chu, X. Zhu, F. Fioranelli, J. Le Kernec, and C. Li "Continuous human motion recognition with a dynamic range-Doppler trajectory method based on FMCW radar," *IEEE Trans. Geosci. Remote Sens.*, vol. 57, no. 9, pp. 6821–6831, Sep. 2019.

[4] S. Jardak, M.-S. Alouini, T. Kiuru, M. Metso, and S. Ahmed, "Compact mmWave FMCW radar: Implementation and performance analysis," *IEEE Aerosp. Electron. Syst. Mag.*, vol. 34, no. 2, pp. 36–44, Feb. 2019.

[5] S. Srivastava and P. Hobden, "5GHz chirp signal generator for broadband FMCW radar applications," in *Proc. IEEE Int. Symp. Smart Electron. Syst. (iSES) (Formerly iNiS)*, Dec. 2018, pp. 152–155.

[6] J. M. S. Macasero, O. J. L. Gerasta, D. P. Pongcol, V. J. V. Ylaya, and A. B. Caberos, "Underground target objects detection simulation using FMCW radar with SDR platform," in *Proc. IEEE 10th Int. Conf. Humanoid, Nanotechnol., Inf. Technol., Commun. Control, Environ. Manage. (HNICEM)*, Nov. 2018, pp. 1–7.

[7] N. F. M. Ariffin, F. N. M. Isa, and A. F. Ismail, "FMCW radar for slow moving target detection: Design and performance analysis," in *Proc. Int. Conf. Comput. Commun. Eng. (ICCCE)*, Jul. 2016, pp. 396–399.

[8] F. Wang, X. Pan, C. Xiang, and M. Chen, "Time-domain algorithm for FMCW based short distance ranging system," in *Proc. 9th Eur. Conf. Antennas Propag. (EuCAP)*, 2015, pp. 1–5.

[9] G. Wang, C. Gu, T. Inoue, and C. Li, "A hybrid FMCW-interferometry radar for indoor precise positioning and versatile life activity monitoring," *IEEE Trans. Microw. Theory Techn.*, vol. 62, no. 11, pp. 2812–2822, Nov. 2014.

[10] I. Kravchenko and V. Vertegel, "An extended simulink model of single-chip automotive FMCW radar," in *Proc. Ural Symp. Biomed. Eng., Radioelectron. Inf. Technol. (USBEREIT)*, Apr. 2019, pp. 368–370.

[11] T. Wang, P. Li, M. Wang, D. Yang, and C. Shi, "A flexible, efficient and low-cost experimental platform for FMCW radars," *Sensor Rev.*, vol. 39, no. 4, pp. 495–503, Jul. 2019.

[12] Y. Ju, Y. Jin, and J. Lee, "Design and implementation of a 24 GHz FMCW radar system for automotive applications," in *Proc. Int. Radar Conf.*, Oct. 2014, pp. 1–4.

[13] E. Hyun, S.-D. Kim, Y.-H. Ju, J.-H. Lee, E.-N. You, J.-H. Park, D.-J. Yeom, S.-H. Park, and S.-G. Kim, "FPGA based signal processing module design and implementation for FMCW vehicle radar systems," in *Proc. IEEE CIE Int. Conf. Radar*, vol. 1, Oct. 2011, pp. 273–275.

[14] E. Hyun, Y.-S. Jin, and J.-H. Lee, "Moving and stationary target detection scheme using coherent integration and subtraction for automotive FMCW radar systems," in *Proc. IEEE Radar Conf. (RadarConf)*, May 2017, pp. 476–481.

[15] H. Ozturk and K. Yegin, "Predistorter based K-band FMCW radar for vehicle speed detection," in *Proc. 17th Int. Radar Symp. (IRS)*, May 2016, pp. 1–4.

[16] E. M. Suijker, R. J. Bolt, M. van Wanum, M. van Heijningen, A. P. M. Maas, and F. E. van Vliet, "Low cost low power 24 GHz FMCW radar transceiver for indoor presence detection," in *Proc. 11th Eur. Radar Conf.*, Oct. 2014, pp. 1758–1761.

[17] B.-S. Oh, X. Guo, and Z. Lin, "A UAV classification system based on FMCW radar micro-Doppler signature analysis," *Expert Syst. Appl.*, vol. 132, pp. 239–255, Oct. 2019.

[18] A. Shoykhetbrod, A. Hommes, and N. Pohl, "A scanning FMCW-radar system for the detection of fast moving objects," in *Proc. Int. Radar Conf.*, Oct. 2014, pp. 1–5.

[19] A. Etinger, N. Balal, B. Litvak, M. Einat, B. Kapilevich, and Y. Pinhasi, "Non-imaging mm-wave FMCW sensor for pedestrian detection," *IEEE Sensors J.*, vol. 14, no. 4, pp. 1232–1237, Apr. 2014.

[20] Y. Xiong, Z. Peng, G. Xing, W. Zhang, and G. Meng, "Accurate and robust displacement measurement for FMCW radar vibration monitoring," *IEEE Sensors J.*, vol. 18, no. 3, pp. 1131–1139, Feb. 2018.
[21] R. Chae, A. Wang, and C. Li, "FMCW radar driver head motion monitoring based on Doppler spectrogram and range-Doppler evolution," in *Proc. IEEE Top. Conf. Wireless Sensors Sensor Netw. (WiSNet)*, Jan. 2019, pp. 1–4.

TAO WANG (Senior Member, IEEE) received the Ph.D. degree from the Universite Catholique de Louvain (UCL), Belgium, in 2012, and the Ph.D. degree from Zhejiang University, China, in 2006. Since February 2013, he has been a Professor with Shanghai University. His current interests include signal processing and control techniques for wireless systems. He was an Associate Editor of *EURASIP Journal on Wireless Communications and Networking*.

PING LI received the B.S. degree in electrical and information engineering from Hangzhou Dianzi University, in 2017. He is currently pursuing the Ph.D. degree with the Shanghai Institute for Advanced Communication and Data Science. His current research interests include radar signal processing and target detection.

RUI WANG (Senior Member, IEEE) received the B.S. and Ph.D. degrees in electronics and information engineering from Xidian University, Xi'an, Shaanxi, China, in 2004 and 2009, respectively. Since 2009, he has been with the School of Communication and Information Engineering, Shanghai University, where he is currently an Associate Professor. His research interests include sensor networks, geometric algebra, and multimedia signal processing.

ZHICHAO SHENG (Member, IEEE) received the Ph.D. degree in electrical engineering from the University of Technology Sydney, Sydney, NSW, Australia, in 2018. From 2018 to 2019, he was a Research Fellow with the School of Electronics, Electrical Engineering and Computer Science, Queen's University Belfast, Belfast, U.K. He is currently an Assistant Professor with Shanghai University, Shanghai, China. His research interests include optimization methods for wireless communication and signal processing.

LIXUN HUANG received the B.S. degree in electronic information science and technology and the M.S. degree in computer application technology from the Henan University of Technology, China, in 2006 and 2009, respectively, and the Ph.D. degree in communication and information system from Shanghai University, China, in 2013. Since July 2013, he has been a Lecturer with the Zhengzhou University of Light Industry. His research interests include iterative learning control and wireless network control.